Dumbbell diffusion in a spatially periodic potential

Jochen Bammert, Steffen Schreiber, and Walter Zimmermann
Theoretische Physik I, Universität Bayreuth, D-95440 Bayreuth, Germany
(Received 2 October 2007; published 21 April 2008)

We present a numerical investigation of the Brownian motion and diffusion of a dumbbell in a two-dimensional periodic potential. Its dynamics is described by a Langevin model including the hydrodynamic interaction. With increasing values of the amplitude of the potential we find along the modulated spatial directions a reduction of the diffusion constant and of the impact of the hydrodynamic interaction. For modulation amplitudes of the potential in the range of the thermal energy the dumbbell diffusion exhibits a pronounced local maximum at a wavelength of about 3/2 of the dumbbell extension. This is especially emphasized for stiff springs connecting the two beads.

DOI: 10.1103/PhysRevE.77.042102 PACS number(s): 05.40.−a, 87.15.Vv, 82.35.Lr

Investigations of the diffusion of different colloidal particles in a homogeneous solvent have a long history [1,2], while studies of the diffusion of small spheres, dimers, and polymers in different potentials attracted considerable interest only for a short time [3–9]. Laser-tweezer arrays are a new powerful tool for generating the desired spatially periodic, correlated, or unstructured potentials in order to study the effects of inhomogeneous potential landscapes on the motion of colloidal particles [3–5,10]. Furthermore, recent studies of dumbbells and polymers in random potentials have created exciting results in statistical physics [11,12].

Several of these investigations are motivated by possible applications like particle sorting in inhomogeneous potentials. For example, cross-streamline migration of colloidal particles has been found in a flow through an optically induced periodic potential. Since this migration depends on the extent of the colloidal particles, the laser-tweezer array has been successfully used for sorting particles with respect to their size [4,10].

We investigate Brownian motion and the diffusion of dumbbells through a two-dimensional periodic potential, which is described by a Langevin model. In doing so we include the effects of the hydrodynamic interaction between the two beads of the dumbbell and focus on the interplay between the dumbbell extension b and the wavelength λ of the spatially periodic potential. In the context of this work the dumbbell may be considered as a simple model for anisotropic colloids [13] pom-pom polymers [14] or two spheres which are connected either by a rather flexible λ-DNA molecule or by a semi-flexible actin filament.

Our numerical studies reveal a significant dependence of the dumbbell diffusion on the ratio λ/b. With the potential amplitude V_0 of the order of the thermal excitation energy k_BT we find a remarkable maximum of the dumbbell diffusion constant in the range of $\lambda \approx 3b/2$. The height of this diffusion maximum increases with the stiffness of the spring connecting the two beads of the dumbbell. Another remarkable effect is the reduction of the influence of the hydrodynamic interaction with increasing potential amplitude.

We describe the Brownian motion of a dumbbell in a two-dimensional periodic potential by the Langevin equation (without inertia)

$$\dot{\mathbf{r}}_i = \mathbf{H}_{ij}(\mathbf{F}_j^{\Phi} + \mathbf{F}_j^{V}) + \mathbf{F}_i^{S} \quad (i,j = 1,2) \tag{1}$$

for the bead positions $\mathbf{r}_i=(x_i,y_i,z_i)$. The linear spring force $\boldsymbol{F}_i^{\Phi}$ between them is determined by the harmonic potential

$$\Phi(\mathbf{r}_1,\mathbf{r}_2) = \frac{k}{2}(b - |\mathbf{r}_1 - \mathbf{r}_2|)^2, \tag{2}$$

with the equilibrium length b of the spring and the corresponding spring constant k. The spatially periodic force $\mathbf{F}_i^{V}=-\boldsymbol{\nabla} V(\mathbf{r}_i)$ is derived from the two-dimensional potential in the xy plane,

$$V(\mathbf{r}_i) = 2V_0 \cos\left(\frac{x_i + y_i}{\lambda}\pi\right)\cos\left(\frac{x_i - y_i}{\lambda}\pi\right), \tag{3}$$

which can be realized in experiments by a laser-tweezer array. Its amplitude V_0 may be changed by varying the intensity of the laser light. The same wavelength λ is chosen in the x and y directions.

In the absence of hydrodynamic interactions (HI) between the beads the mobility matrix $\mathbf{H}$ is a diagonal matrix ($\mathbf{H}_{ii}=\frac{1}{\zeta}\mathbf{I}$, $\mathbf{H}_{ij}=0$ for $i \neq j$) being inversely proportional to the Stokes friction coefficient $\zeta=6\pi\eta a$ which depends on the solvent viscosity η as well as on the effective hydrodynamic bead radius a. The HI between the two beads is taken into account by the Rotne-Prager tensor [15] where the mobility matrix for $i \neq j$ has the following structure:

$$\mathbf{H}_{ij} = \frac{1}{8\pi\eta r_{ij}}\left[\left(1 + \frac{2}{3}\frac{a^2}{r_{ij}^2}\right)\mathbf{I} + \left(1 - 2\frac{a^2}{r_{ij}^2}\right)\hat{\mathbf{r}}_{ij}\hat{\mathbf{r}}_{ij}^T\right]. \tag{4}$$

Note that $\mathbf{r}_{ij}=\mathbf{r}_i-\mathbf{r}_j$ is the distance vector between the beads and r_{ij} is its norm.

The stochastic forces $\mathbf{F}_i^S$ caused by the thermal heat bath are related to the dissipative drag by the fluctuation dissipation theorem which ensures the correct equilibrium properties. They can be combined to a single supervector $\mathbf{F}^S=(\mathbf{F}_1^S,\mathbf{F}_2^S)$, which reads

$$\mathbf{F}^S = \sqrt{2k_BT\mathbf{H}}\boldsymbol{\xi}. \tag{5}$$

T is the temperature, k_B the Boltzmann constant, and $\boldsymbol{\xi}(t)$ is the uncorrelated Gaussian white-noise vector with zero mean and unit variance:

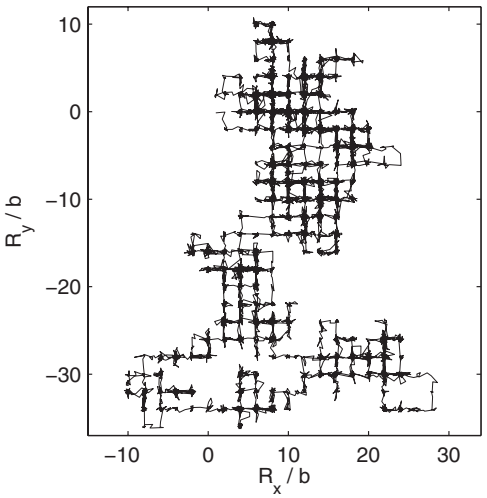

FIG. 1. The trajectory of the c.m. of the dumbbell in the xy plane follows predominantly along the saddles between the minima of the potential. Parameters: $k=10$, $V_0/k_BT=2$, and $\lambda=2b$.

$$\langle \boldsymbol{\xi}(t) \rangle = 0, \tag{6}$$

$$\langle \boldsymbol{\xi}(t) \boldsymbol{\xi}^T(t') \rangle = \delta(t-t')\mathbf{l}. \tag{7}$$

The fixed parameters in our simulations are $b=1$ for the typical length scale and $k_BT=1$ which determines the energy scale. If not stated otherwise, we use $\frac{a}{b}=\frac{1}{5}$, $\eta=1$. k determines the binding energy of the spring in units of the thermal energy $\frac{kb^2}{k_BT}$. Most of our results were observed after averaging over more than 10^4 ensembles.

A typical trajectory of the center of mass (c.m.) of the dumbbell, $\mathbf{R}=(\mathbf{r}_1+\mathbf{r}_2)/2$, in the xy plane is shown in Fig. 1 for $k=10$, $\lambda=2b$, and $V_0=2k_BT$. It passes the saddles between the maxima of the potential, and accordingly the trajectory adapts to the quadratic structure of the potential landscape. If one of the two parameters k or λ/b is reduced, larger excursions of the c.m. away from the potential minima occur and more diagonal jumps between the valleys are found.

The mean-square displacement $\langle R_l^2(t) \rangle = 2D_l t$ $(l=x,y,z)$ increases linearly in time along each spatial direction as shown for one parameter set in Fig. 2. This behavior is typical for normal diffusion. Parallel to the z direction one has an undisturbed diffusion and therefore the mean-square displacement and thus D_z are much larger than in the modulated x and y directions. Along these two directions the saddles and the local maxima between neighboring potential valleys act as barriers for the dumbbell motion and therefore D_x (equal to D_y) is smaller than D_z. Moreover, for a dumbbell in a solvent the HI between the two beads comes into play, which in general enhances the diffusion as can be seen by the shift between the solid and dashed lines in Fig. 2.

The decay of the dumbbell diffusion as a function of the ratio between the modulation amplitude of the potential and the thermal energy V_0/k_BT is shown in Fig. 3 for one parameter set with HI (solid line) and without HI (dashed line) between the beads. The decay of D_x is similar to the results described in Refs. [6,7] on the diffusion of point like particles. The difference between the two cases with and without HI is shrinking with an increasing modulation amplitude of the potential, because the higher diffusivity caused by HI becomes less important with increasing potential barriers. Accordingly, the ratio D_x/D_z between the diffusion along one modulated direction and the unmodulated direction is smaller with HI than for the case without HI, as shown in Fig. 3.

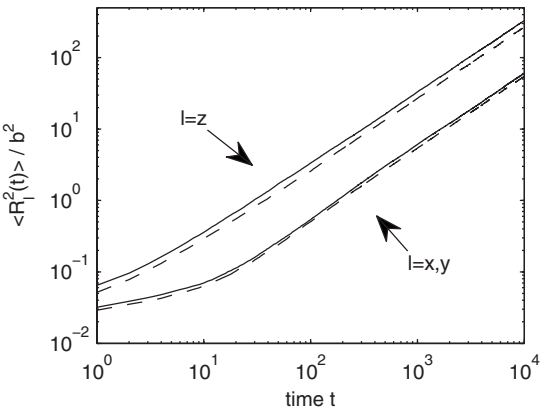

FIG. 2. The mean-square displacement of the c.m. of the dumbbell is shown along the x and y directions (lower lines) and along the z direction (upper lines) with HI between the beads (solid lines) and without (dashed lines). The parameters are the same as in Fig. 1.

In contrast to the diffusion of point particles the diffusion of a dumbbell along one modulated direction also depends on the interplay between the two length scales: namely, the bead distance b and the wavelength λ of the periodic potential modulation. A typical functional dependence of the dumbbell diffusion on the ratio λ/b is shown in Fig. 4, where the diffusion is remarkably enhanced for λ close to $\lambda_1=3b/2$. Further beyond this value the dumbbell diffusion decreases with increasing values of the wavelength up to a minimum $D_x(\lambda_2)$, which is at about $\lambda_2 \approx 6b$ for the given parameters (not shown in Fig. 4). The decay of D_x in the range $\lambda_1 < \lambda < \lambda_2$ can be explained in the following way. For increasing values $\lambda \gtrsim \lambda_1$ the beads become essentially caged within one single potential valley and an escape from such a

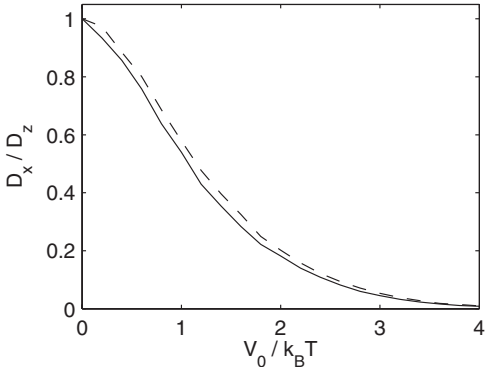

FIG. 3. The diffusion D_x $(=D_y)$ in the x direction is normalized by the free diffusion D_z in the z direction and plotted as a function of V_0/k_BT for the case with HI (solid line) and without HI (dashed line). The following parameters have been used: $k=10$ and $\lambda=2b$.

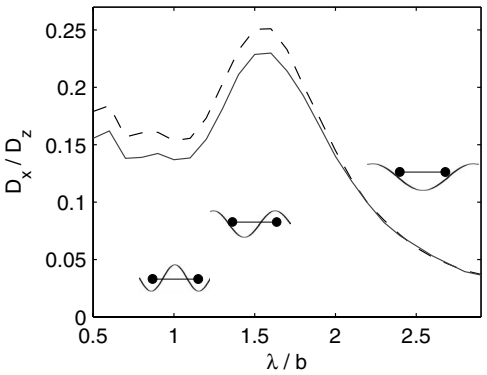

FIG. 4. The normalized diffusion constant D_x/D_z $(=D_y/D_z)$ of the dumbbell is shown as a function of the ratio between the equilibrium bead distance b and the wavelength λ for the case with HI (solid line) and without HI (dashed line). The insets illustrate possible locations of the dumbbell with respect to the periodic potential for different values of λ/b. The parameters are $V_0/k_BT=2$ and $k=10$.

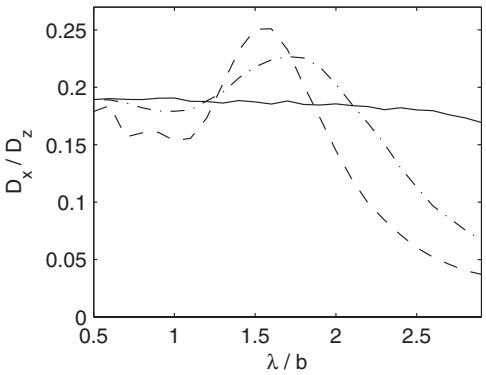

FIG. 5. The ratio between the diffusion constants D_x/D_z of the dumbbell is shown for three different values of the spring constant (solid line, $k=0.1$; dash-dotted line, $k=1$; dashed line, $k=10$) as a function of the ratio λ/b. The potential amplitude is $V_0=2k_BT$.

trap gets more and more unlikely (see right inset in Fig. 4). If the wavelength λ is increased further beyond λ_2, the mean-square displacement and the dumbbell diffusion increase again and finally approach the value of the unmodulated case, because for large wavelengths the dumbbell does not feel the potential anymore.

If on the other hand the modulation wavelength is reduced below λ_2, the distance from the potential minimum to a saddle is shortened. In such a case it becomes more likely that the dumbbell is kicked over a saddle to a neighboring potential valley. So the diffusion D_x increases with decreasing values in the range $\lambda_1<\lambda<\lambda_2$.

Near the maximum of the diffusion constant at $\lambda\approx\lambda_1$ an additional effect comes into play which supports a dumbbell movement from one potential valley to another and accordingly enhances the dumbbell diffusion. In this range the two beads hardly fit into one single potential valley as indicated by the middle inset in Fig. 4. Moreover, for a rather stiff spring both beads cannot reach the minima of two neighboring potential valleys simultaneously. So the required excitation energy is smaller than V_0 and for this reason the diffusive motion is enhanced.

In the range $\lambda\leq b$ the dumbbell easily finds an orientation in the potential plane where the two beads are located in two distinct minima; cf. the left inset of Fig. 4. Only one bead needs to be kicked to another valley in order to make progress for the c.m. of the dumbbell. Therefore, irrespective whether the two beads belong to nearest neighbor valleys or not, the required excitation energy for a shift of the c.m. depends only weakly on λ. This is the origin of the small variations of D_x in the range $\lambda<b$.

The explanation given for the local maximum of the diffusion constant in the range of λ_1 in Fig. 4 is supported by the influence of the spring constant k on the height of $D_x(\lambda_1)$ and on the mean distance $\langle r_{12}\rangle$. The local maximum of D_x is especially pronounced in the case of a rather stiff dumbbell (see Fig. 5) where the distribution of the bead distance $\rho(r_{12})$ is not changed by the periodic potential (see Fig. 6). On the other hand, for smaller values of k the maximum of $\rho(r_{12})$ is more and more shifted from b to λ. In this case the beads relax down to the potential valleys, so a higher excitation energy is required for a shift of the c.m., which results in a smaller diffusion constant as indicated by the solid line in Fig. 5.

The distance between the potential valleys depends on the direction in the xy plane, and therefore the orientational distribution of the dumbbell axis $\rho(\Phi)$ in Fig. 7 provides a complementary piece of information to $\rho(r_{12})$. The two beads of the dumbbell may relax more easily to the potential minima in the case of a soft spring (cf. solid lines in Fig. 7) compared to a stiff spring (cf. dashed lines). So the orientational distribution of the dumbbell axis in the xy plane shows, besides the maxima along the x and y directions, a local maximum for a diagonal orientation of the dumbbell axis. This is displayed in Fig. 7(a). If the wavelength is reduced to $\lambda=b$, one finds, in addition to the maximum in the diagonal direction (11), local maxima along the (21) and (12) directions, as indicated by Fig. 7(b).

The Brownian motion of a dumbbell in a two-dimensional periodic potential has been investigated in terms of a

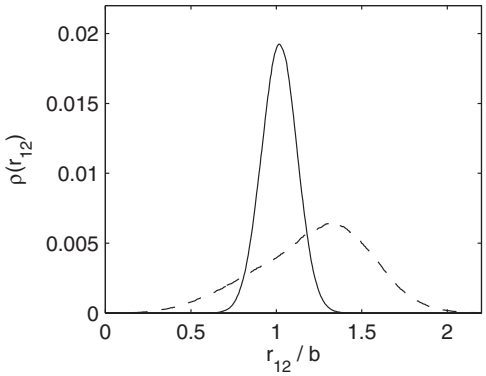

FIG. 6. The distribution $\rho(r_{12})$ of the bead distances is shown for two different values of the spring constant, $k=10$ (solid line) and $k=1$ (dashed line), and for the parameters $V_0/k_BT=2$ and $\lambda/b=3/2$.

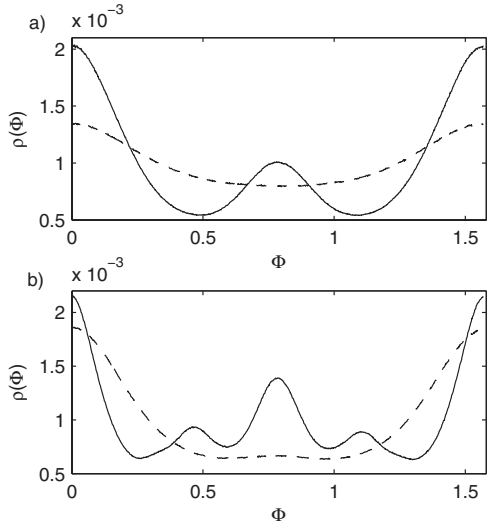

FIG. 7. The orientational distribution $\rho(\Phi)$ of the dumbbell axis in the xy plane is shown for two different values of the spring constant (solid line, $k=1$; dashed line, $k=10$) and for $V_0/k_BT=2$. The angle Φ is measured with respect to the x axis, and the ratio between the wavelength λ and the bead distance b is (a) $\lambda/b=2$ and (b) $\lambda/b=1$.

Langevin model. For an increasing barrier height between the potential minima, we find a decreasing diffusion constant for the center of mass along the modulated spatial directions as well as a reduction of the influence of the hydrodynamic interaction. For stiff springs the diffusion additionally depends on the ratio between the wavelength λ of the potential modulation and the equilibrium dumbbell extension b. In the range $\lambda \approx 3b/2$ this interplay is especially pronounced, because the two beads do not fit into one single or two neighboring potential minima anymore and this mismatch causes a reduced effective barrier height and thus an enhanced diffusion constant. If the spring constant is small, the beads can relax down to the potential minima over a wide range of λ, which results in a diffusion constant that is rather independent from λ in this domain. So the height of the maximum of the diffusion constant at $\lambda \approx 3b/2$ increases with the spring stiffness. For modulation wavelengths further beyond $3b/2$ the diffusion constant decays monotonically until some minimum is reached. In this range the dumbbell is essentially caged in one single potential valley and it is rather unlikely that it escapes. Beyond this minimum as λ goes to infinity the diffusion constant grows until the free diffusion limit is reached.

According to the dependence of the dumbbell diffusion on the ratio λ/b different values of the modulation wavelength λ in x and y directions cause an anisotropic diffusion behavior. In addition, the results presented may be useful for sorting polydisperse particle mixtures with respect to the particles' elasticity and size.

We would like to thank L. Holzer for instructive discussions. This work has been supported by the German Science Foundation through the priority program on micro- and nanofluidics No. SPP 1164.

[1] M. Doi and S. F. Edwards, *The Theory of Polymer Dynamics* (Clarendon Press, Oxford, 1986).
[2] A. Einstein, Ann. Phys. **17**, 549 (1905).
[3] P. T. Korda, M. B. Taylor, and D. G. Grier, Phys. Rev. Lett. **89**, 128301 (2002).
[4] M. P. MacDonald, G. C. Spalding, and K. Dholakia, Nature (London) **426**, 421 (2003).
[5] K. Ladavac, K. Kasza, and D. G. Grier, Phys. Rev. E **70**, 010901(R) (2004).
[6] A. H. Romero, A. M. Lacasta, and J. M. Sancho, Phys. Rev. E **69**, 051105 (2004).
[7] A. M. Lacasta, J. M. Sancho, A. H. Romero, and K. Lindenberg, Phys. Rev. Lett. **94**, 160601 (2005).
[8] C. Fusco and A. Fasolino, ChemPhysChem **6**, 1749 (2005).
[9] R. Tsekov and E. Ruckenstein, Surf. Sci. **344**, 175 (1995).
[10] Y. Roichman, V. Wong, and D. G. Grier, Phys. Rev. E **75**, 011407 (2007).
[11] V. G. Rostiashvili and T. A. Vilgis, J. Chem. Phys. **120**, 7194 (2004).
[12] M. Schulz, S. Stepanov, and S. Trimper, Europhys. Lett. **54**, 424 (2001).
[13] P. M. Johnson, C. M. van Kats, and A. van Blaaderen, Langmuir **21**, 11510 (2005).
[14] T. C. B. McLeish and R. G. Larson, J. Rheol. **42**, 81 (1998).
[15] J. Rotne and S. Prager, J. Chem. Phys. **50**, 4831 (1969).